Note Added in Proof. Since Tl(II) has been suggested to one-electron oxidize 9-methylguanine,[19] this reagent was used (as a third oxidant) with guanosine, and the reaction was monitored with conductance in the pH range 3–6. At pH 3 (where the oxidizing species is Tl^{2+}),[39] the reaction led to removal of 1 equiv of H^+, whereas at pH 6 (where the oxidizing species is $TlOH^+$),[39] the net change of $[H^+]$ was zero.[40] The inflection point of the conductance vs pH plot was 3.9, in perfect agreement with the pK_a value of $G^{\bullet+}$ as determined by using $Br_2^{\bullet-}$ or $SO_4^{\bullet-}$ as oxidants. The observations are described by, at pH 6,

$$OH^\bullet + Tl^+ \rightarrow TlOH^+$$

$$TlOH^+ + G \rightarrow Tl^+ + H_2O + G(-H)^\bullet$$

at pH 3,

$$OH^\bullet + Tl^+ + H^+ \rightarrow Tl^{2+} + H_2O$$

$$Tl^{2+} + G \rightarrow Tl^+ + G^{\bullet+}$$

and eq 3.

---

[39] O'Neill, P.; Schulte-Frohlinde, D. *J. Chem. Soc., Chem. Commun.* **1975**, 387.

[40] The reaction of Tl^{2+} with anisole (≡100%)[28] was used for calibration. On this basis, Tl(II) reacts with guanosine quantitatively by electron transfer.

Registry No. $SO_4^{\bullet-}$, 12143-45-2; $Br_2^{\bullet-}$, 12595-70-9; deoxyguanosine, 961-07-9; guanosine, 118-00-3; 1-methylguanosine, 2140-65-0.

Chemically Induced Release of Charge from a Rectifying Polymer Based on Viologen and Quinone Subunits

Diane K. Smith, Leonard M. Tender, Gregg A. Lane, Stuart Licht, and Mark S. Wrighton*

Contribution from the Department of Chemistry, Massachusetts Institute of Technology, Cambridge, Massachusetts 02139.

Received June 3, 1988.
Revised Manuscript Received September 8, 1988

Abstract: Charge associated with the reduction of quinone, $2e^- + 2H^+ + Q \rightarrow QH_2$, can be trapped at low pH in the electrode-confined siloxane polymer, $(BV\text{-}Q\text{-}BV^{6+})_n$, which is derived from a monomer that consists of a benzoquinone unit flanked by two benzyl viologen units. $2ne^-$'s can be released from the polymer by raising the solution pH to neutral or basic pH where the viologen can reoxidize the QH_2 to Q, ultimately delivering the charge to the electrode. Chemical redox reagents, added to the polymer film, can also be used to release the charge and deliver it to the electrode. The use of I_3^-/I^- and $Fe(CN)_6^{3-/4-}$ as charge-release mediators is demonstrated. Oxidation of QH_2 centers occurs when the potential of an electrode modified with $(BV\text{-}Q\text{-}BV^{6+})_n$ is brought close to $E°'(I_3^-/I^-)$ or $E°'(Fe(CN)_6^{3-/4-})$. Because $Fe(CN)_6^{3-/4-}$ is concentrated by the polycationic $(BV\text{-}Q\text{-}BV^{6+})_n$ polymer, only very small solution concentrations, approximately 1 μM, are required to effectively mediate the oxidation of QH_2.

In this article we describe chemical mechanisms that can be used to release charge trapped in an electrode-confined, rectifying, redox polymer. In particular, we show that a variation in pH from low to high results in delivery of charge to the electrode. In addition, we show that certain solution redox additives can serve as mediators to deliver charge to the electrode. The significance of this work is 2-fold: (1) we demonstrate a system where a pH change brings about a thermodynamically allowed electrochemical process converting the chemical change to an electric current, and (2) we demonstrate that the rectifying properties of a polymer film can be rationally altered by judicious choice of charge-release agents added to the rectifying film.

This work continues the characterization of the electrode-confined polymer, $(BV\text{-}Q\text{-}BV^{6+})_n$, derived from base hydrolysis of the pendant trimethoxysilyl units on **1**.[1] Electrode surfaces modified with $(BV\text{-}Q\text{-}BV^{6+})_n$ undergo a $4ne^-/2nH^+$ reduction between pH 9 and 1 upon moving the potential from +0.2 to −0.7 V vs SCE. This corresponds to $2n$ 1e reductions of the viologen units, BV^{2+}, to the radical cationic form, BV^+, and n $2e^-/2H^+$ reductions of the quinone centers, Q, to the hydroquinone form, QH_2 (eq 1). The interesting observation is that while the reduction is completely reversible above pH 6, only the $2ne^-$ in the viologen system can be removed electrochemically below pH 6, even when the electrode is held substantially positive of the Q/QH_2

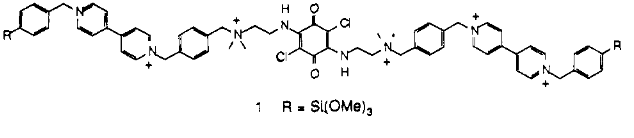

1 R = Si(OMe)$_3$

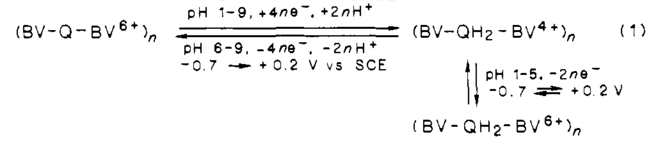

$$\begin{tikzcd}[column sep=huge] (BV\text{-}Q\text{-}BV^{6+})_n \arrow[r, shift left, "\substack{+0.2 \rightarrow -0.7 \text{ V vs SCE} \\ \text{pH } 1-9,\ +4ne^-,\ +2nH^+}"] & (BV\text{-}QH_2\text{-}BV^{4+})_n \arrow[l, shift left, "\substack{\text{pH } 6-9,\ -4ne^-,\ -2nH^+ \\ -0.7 \rightarrow +0.2 \text{ V vs SCE}}"] \arrow[d, shift left, "\substack{\text{pH } 1-5,\ -2ne^- \\ -0.7 \rightleftarrows +0.2 \text{ V}}"] \\ & (BV\text{-}QH_2\text{-}BV^{6+})_n \arrow[u, shift left] \end{tikzcd} \quad (1)$$

---

[1] (a) Smith, D. K.; Lane, G. A.; Wrighton, M. S. *J. Am. Chem. Soc.* **1986**, *108*, 3522. (b) Smith, D. K.; Lane, G. A.; Wrighton, M. S. *J. Phys. Chem.* **1988**, *92*, 2616.

0002-7863/89/1511-1099$01.50/0 © 1989 American Chemical Society

Scheme I. Base-Induced Change in Energetics Resulting in Charge Release from $(BV\text{-}QH_2\text{-}BV^{6+})_n$

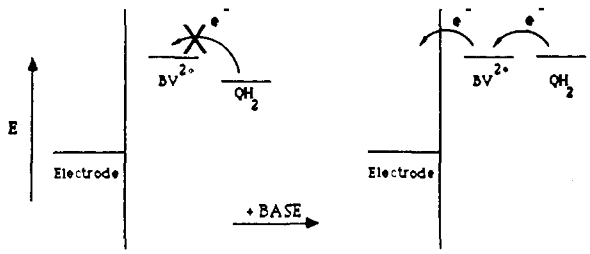

(a) Low pH (b) High pH

redox potential. Thus, charge in the form of QH_2 is "trapped" in the polymer at acidic pH's.

The charge-trapping property of $(BV\text{-}QH_2\text{-}BV^{6+})_n$ is analogous to what Murray and co-workers have observed using bilayer assemblies of redox polymers.[2] These electrodes are designed to trap charge by choosing polymers with appropriately ordered redox potentials. For example, the inner layer may have a reduction potential more negative than the outer layer, so when the inner layer is reduced, the electrons flow quickly into the outer layer, an energetically "downhill" process. The electrons in the outer layer are kinetically trapped, because in order to return to the electrode they must surmount the energy barrier between outer and inner layers, even when the electrode is held at a potential where the electrons should thermodynamically return to the electrode.

$(BV\text{-}Q\text{-}BV^{6+})_n$-modified electrodes behave in a manner similar to bilayer electrodes because the Q centers, like the outer layer polymer in a bilayer, are unable to directly equilibrate with the electrode. This inability is partly due to structural constraints, as in the bilayer, but also due to inherently slow Q/QH_2 self-exchange rates.[3] However, although the Q centers cannot directly equilibrate with the electrode, the electrochemical reduction of Q centers and oxidation of QH_2 centers can be mediated by $BV^{2+/+}$. $BV^{2+/+}$, therefore, serves the same function in $(BV\text{-}Q\text{-}BV^{6+})_n$ as the inner layer in a bilayer. At neutral and basic pH's, the formal redox potential, $E°'$, of $BV^{2+/+}$ (−0.4 V vs SCE) is close enough to that of Q/QH_2 (−0.4 V vs SCE at pH 9) that the $BV^{2+/+}$ units can mediate both reduction and oxidation of the Q/QH_2 centers. However, at lower pH, $E°'(Q/QH_2)$ shifts positive. Between pH 6 and 5, $E°'(Q/QH_2)$ is sufficiently positive of $E°'(BV^{2+/+})$ that BV^{2+} can no longer oxidize QH_2. When this happens, the Q centers in $(BV\text{-}Q\text{-}BV^{6+})_n$ can be reduced electrochemically via $BV^{2+/+}$ mediation, but QH_2 cannot be oxidized.

In this paper we report several methods that can be used to release charge trapped in $(BV\text{-}QH_2\text{-}BV^{6+})_n$ at acidic pH. In the bilayer assemblies studied by Murray and co-workers, trapped charge can be released electrochemically by accessing another redox level in the inner layer.[2] This is not possible with $(BV\text{-}QH_2\text{-}BV^{6+})_n$ because the viologen units do not possess a more positive stable oxidation state than BV^{2+}. More indirect methods must therefore be investigated. The first method examined was a pH jump. Charge trapped at acidic pH can be released by raising the solution pH to a value where QH_2 can be oxidized via the $BV^{2+/+}$ system (Scheme I). This technique was used by Meyer and co-workers to release charge trapped in a bilayer having a pH-dependent redox couple in the outer layer.[4]

Scheme II. Release of Trapped Charge from $(BV\text{-}QH_2\text{-}BV^{6+})_n$ by Use of a Mobile Mediator, M, to Oxidize QH_2

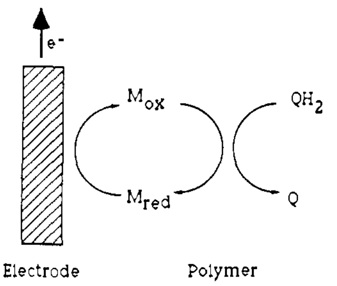

It should be pointed out that changing the pH can generally result in a current flow for a potentiostated electrode modified with a pH-dependent redox couple. The key difference conveyed in Scheme I is that the electrode is held at a potential thermodynamically capable of accepting charge from QH_2. The chemical signal, therefore, needs, in principle, to only be *catalytic*.

A general method illustrating catalytic charge release from $(BV\text{-}QH_2\text{-}BV^{6+})_n$ is to add an additional redox system that can mediate the oxidation of QH_2 by accepting charge (electrons) from QH_2 and delivering the charge to the electrode (Scheme II). The use of redox mediators allows manipulation of the rectifying properties of $(BV\text{-}Q\text{-}BV^{6+})_n$, since the additives control the potential where trapped charge will be released. Two mediator systems for $(BV\text{-}Q\text{-}BV^{6+})_n$ have been investigated: I_3^-/I^- and $Fe(CN)_6^{3-/4-}$. The reduced form of these species can be added to the solution with little or no effect on the electrochemistry of the $BV^{2+/+}$ and Q/QH_2 polymer subunits. Electrochemical oxidation of QH_2 centers, releasing trapped charge, occurs when the electrode is brought near $E°'(I_3^-/I^-)$ or $E°'(Fe(CN)_6^{3-/4-})$. The $Fe(CN)_6^{3-/4-}$ system has been examined in greatest detail. This system is particularly interesting, because small amounts of $Fe(CN)_6^{3-/4-}$ in solution will concentrate in the polycationic polymer. This means that only very small solution concentrations of $Fe(CN)_6^{3-/4-}$ are needed to effectively mediate charge release. Significant work has already been reported on the use of mobile redox mediators for equilibrating the Q/QH_2 couple in a polymer film.[5]

Experimental Section

Chemicals. **1** was prepared as previously reported.[1] Electrolyte solutions were prepared with glass-distilled H_2O (Omnisolve, EM Science). pH 7.2 solutions were buffered with 0.1 M tris(hydroxymethyl)aminomethane/HCl (Tris); pH 1.2 solutions were prepared from 0.1 M ultrapure H_2SO_4 (Ultrex, Baker).

Electrode Fabrication and Derivatization. Glassy-carbon electrodes were prepared with 3-mm diameter glassy-carbon rod (Atomergic Chemetals). Pieces of glassy carbon (1 cm long) were embedded in clear epoxy (Hysol) and sealed in glass tubing with white epoxy (Hysol). The surface was polished with successively finer grades of emory paper, followed by polishing with 6- and 3-μm diamond paste (Metadi II, Buehler). Commercial glassy-carbon electrodes (Bioanalytical Systems) were also used. Before derivatization, both types of electrodes were polished with 1-μm γ-Al_2O_3 and then 0.05-μm deagglomerated γ-Al_2O_3 (Micropolish II, Buehler).

Electrodes were derivatized with $(BV\text{-}Q\text{-}BV^{6+})_n$ by holding at −0.7 V vs SCE in a ~5 mM solution of **1** in aqueous 0.2 M KCl/0.1 M K_2HPO_4 until the desired coverage was achieved. The electrodes were then soaked for at least 12 h in 1.0 M KCl/pH 7.2 Tris buffer before use.

Electrochemical Equipment and General Procedures. Electrochemical experiments were performed on either a PAR Model 363 potentiostat/galvanostat and PAR Model 175 universal programmer or a Pine Model RDE4 bipotentiostat, with either a Houston Instruments Model 2000 X-Y recorder or a Kipp and Zonan BD91 X-Y-Y′ recorder. Rotating-disk experiments were performed on a Pine Model MSR rotator. A Nicolet Model 4094B digital oscilloscope was used to record data in the potential-step experiments.

---

[2] (a) Leidner, C. R.; Murray, R. W. *J. Am. Chem. Soc.* **1985**, *107*, 551. (b) Pickup, P. G.; Kutner, W.; Leidner, C. R.; Murray, R. W. *J. Am. Chem. Soc.* **1984**, *104*, 1991. (c) Pickup, P. G.; Leidner, C. R.; Denisevitch, P.; Murray, R. W. *J. Electroanal. Chem. Interfacial Electrochem.* **1984**, *164*, 39. (d) Leidner, C. R.; Denisevich, P.; Willman, K. W.; Murray, R. W. *J. Electroanal. Chem. Interfacial Electrochem.* **1984**, *164*, 63. (e) Schneider, J. R.; Murray, R. W. *Anal. Chem.* **1982**, *54*, 1508. (f) Willman, K. W.; Murray, R. W. *J. Electroanal. Chem. Interfacial Electrochem.* **1982**, *133*, 211. (g) Denisevich, P.; Willman, K. W.; Murray, R. W. *J. Am. Chem. Soc.* **1981**, *103*, 4727. (h) Denisevich, P.; Willman, K. W.; Murray, R. W. *J. Am. Chem. Soc.* **1981**, *103*, 4727.

[3] Laviron, E. *J. Electroanal. Chem. Interfacial Electrochem.* **1986**, *208*, 357; **1984**, *169*, 29.

[4] Vining, W. J.; Surridge, N. A.; Meyer, T. J. *J. Phys. Chem.* **1986**, *90*, 2281.

[5] Degrand, C.; Roullier, L.; Miller, L. L.; Zinger, B. *J. Electroanal. Chem. Interfacial Electrochem.* **1984**, *178*, 101.

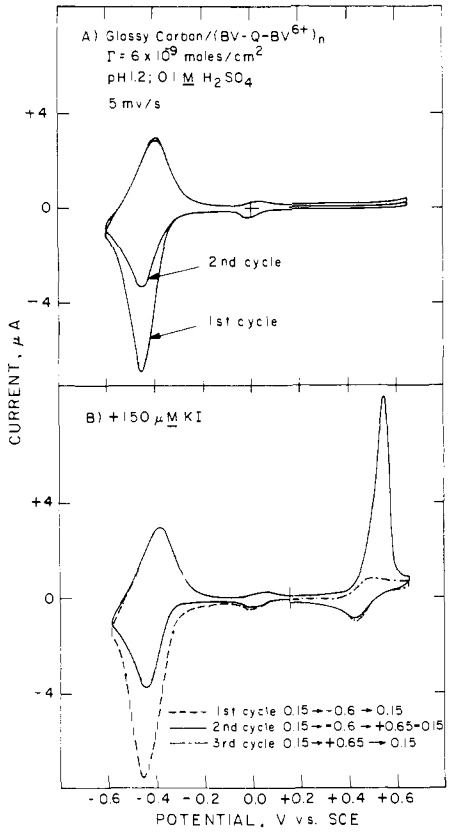

Figure 1. (A) Cyclic voltammetry of a C/(BV-Q-BV^{6+})$_n$ electrode in pH 1.2/0.1 M H$_2$SO$_4$. (B) Demonstration of charge release mediated by I$_3^-$/I$^-$ in the solution. Cyclic voltammetry of the same electrode used in (A) under the same conditions except with 150 μM KI present.

All electrochemical experiments were carried out under N$_2$ or Ar in a one-compartment cell using a standard three-electrode configuration with Pt counter electrode and saturated calomel, SCE, reference electrode.

pH Jump Experiments. Experiments to test whether trapped charge could be released from (BV-QH$_2$-BV^{6+})$_n$ reproducibly via an abrupt change in solution pH were performed by two different methods. In the first method the pH change was accomplished by injecting a small amount of strong base into the acidic electrolyte solution. Specifically, a (BV-Q-BV^{6+})$_n$-modified glassy-carbon rotating-disk electrode was rotated at 1000 rpm in 10 mL of deoxygenated 0.1 M H$_2$SO$_4$, and the current vs time response was monitored as the electrode potential was stepped from +0.2 to -0.6 V and back to +0.2 V vs SCE. Then a small amount of deoxygenated 2 M KOH was injected into the top of the solution. This technique produces a local pH change at the electrode surface sufficiently large to release trapped charge, even though the final pH of the bulk solution can vary considerably. In order to achieve reproducible results, it is necessary to minimize obstructions to solution flow by positioning the reference and counter electrodes carefully and by injecting the base smoothly and in the direction of the flow.

An abrupt change in solution pH was also achieved with a flowing-stream cell. The inlet of the cell was connected to a two-way stopcock, which in turn was connected via PVC tubing to two different reservoirs, one containing Ar-purged acidic electrolyte (buffered at pH 1.2 with 0.1 M H$_2$SO$_4$ or pH 4 with acetate buffer) and the other containing Ar-purged neutral electrolyte (buffered at pH 7.2 with Tris buffer). Flow through the cell was maintained by siphon and the pH jump achieved by turning the stopcock to change the flow source from the acid reservoir to the neutral reservoir.

Results and Discussion

Charge Trapping at pH 1.2 and Charge Release via a pH Jump. The charge trapping ability of (BV-QH$_2$-BV^{6+})$_n$ at acidic pH is illustrated in Figure 1A by a cyclic voltammogram of a glassy-carbon electrode derivatized with (BV-Q-BV^{6+})$_n$ at pH 1.2. Initially, the polymer is in the fully oxidized (BV-Q-BV^{6+})$_n$ state. Starting at +0.65 V vs SCE and scanning negative, the first feature is a small wave at 0 V. This is the expected potential for Q reduction at pH 1.2. However, the area of the wave represents only a small fraction of the Q that is actually present. We interpret the wave as representing the fraction of Q that equilibrates directly with the electrode surface.[1] The majority of the Q is not reduced until ~-0.4 V, which is the potential for reduction of BV^{2+} centers. The return scan (from -0.60 to +0.65 V vs SCE) shows waves for oxidation of all BV$^+$ and the small fraction of QH$_2$ in direct equilibrium with the electrode. However, the return scan shows no current for oxidation of the bulk QH$_2$, even when the electrode is scanned to +0.65 V, well positive of $E°'$(Q/QH$_2$). A second cycle (+0.65 to -0.60 V vs SCE) shows only the wave for the small amount of Q near the electrode and a wave for the BV$^{2+/+}$ system, confirming that the excursion to +0.65 V in the first cycle leaves the bulk of the QH$_2$ fully reduced.

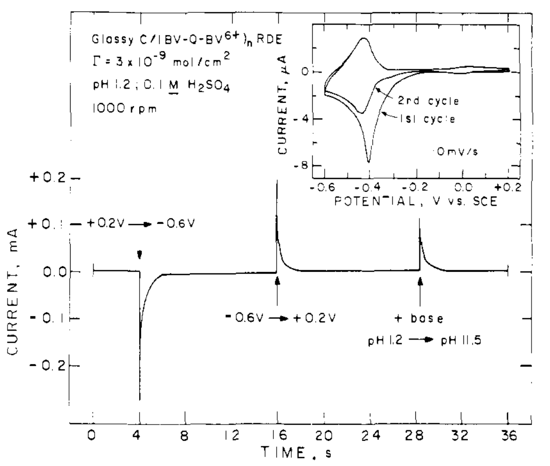

Figure 2. Demonstration of charge release by a pH jump. Current–time profile for a C/(BV-Q-BV^{6+})$_n$ rotating-disk electrode in pH 1.2/0.1 M H$_2$SO$_4$. The electrode is initially in the fully oxidized BV-Q-BV^{6+} state at +0.2 V vs SCE. The potential is then stepped to -0.6 V, producing the 4ne$^-$/2nH$^+$-reduced BV-QH$_2$-BV^{4+} state, and then back to +0.2 V, producing the charge-trapped BV-QH$_2$-BV^{6+} state. Finally, base is added to release the trapped charge. The inset shows the cyclic voltammetry of the electrode in the starting pH 1.2 solution, demonstrating that the electrode used shows typical rectification.

One way to release charge stored in (BV-QH$_2$-BV^{6+})$_n$ is to raise the pH of the solution. This moves the redox potential of Q/QH$_2$ closer to that of BV$^{2+/+}$, allowing oxidation of QH$_2$ centers via mediation by the BV$^{2+/+}$ system. This is demonstrated in Figure 2 with a C/(BV-Q-BV^{6+})$_n$ rotating-disk electrode in pH 1.2 electrolyte. Initially, the polymer is in the fully oxidized state with the potential of the electrode held at +0.2 V vs SCE. The potential is then stepped to -0.6 V, producing a cathodic current transient in a plot of current vs time. This corresponds to the 4ne$^-$/2nH$^+$ reduction of the polymer to the (BV-QH$_2$-BV^{4+})$_n$ state. The electrode is then stepped back to +0.2 V vs SCE, producing an anodic current transient, which corresponds to the formation of the partially oxidized (by 2ne$^-$), charge-trapped (BV-QH$_2$-BV^{6+})$_n$ state. As expected, the area under the anodic current peak is half that under the cathodic current peak. Addition of base produces a second anodic current transient of area equal to that accompanying the -0.6 to +0.2 V step. The pH increase thus results in oxidation of the polymer back to the initial, fully oxidized (BV-Q-BV^{6+})$_n$ state. The results establish the charge release mechanism illustrated in Scheme I.

pH jump experiments have also been done with a flowing-stream cell connected via a two-way stopcock to two reservoirs, one containing acidic electrolyte solution and the other containing neutral electrolyte solution. Charge release from (BV-QH$_2$-BV^{6+})$_n$ was accomplished in this case by simply switching the flow source from the low-pH reservoir to the high-pH reservoir. This method for achieving an abrupt pH change has the advantage over the first method in that the bulk pH change is reproducible and it is easier to repeat the experiment several times with the same electrode in order to check the reproducibility of the charge release. The results of such an experiment are listed in Table I. Although there was a slight decline in electrode coverage over the course

Table I. Charge Trapped with a C/(BV-Q-BV^{6+})$_n$ Electrode at pH 1.2 and Released via a "pH Jump" to pH 7.2[a]

trial	Γ(BV-Q-BV^{6+})$_n$ × 10^9, mol/cm^2	charge trapped[b] × 10^5, C	charge released × 10^5, C
1	5.2	7.4	7.1
2	4.4	6.3	5.2
3	4.5	7.1	5.2
4	4.0	6.0	4.6
5	3.5	4.9	4.4

[a] The pH jumps were performed with the flowing-stream method. See the Experimental Section. [b] Determined by subtracting the charge required to oxidize the BV$^+$ at low pH from the charge required to completely reduce both BV^{2+} and Q.

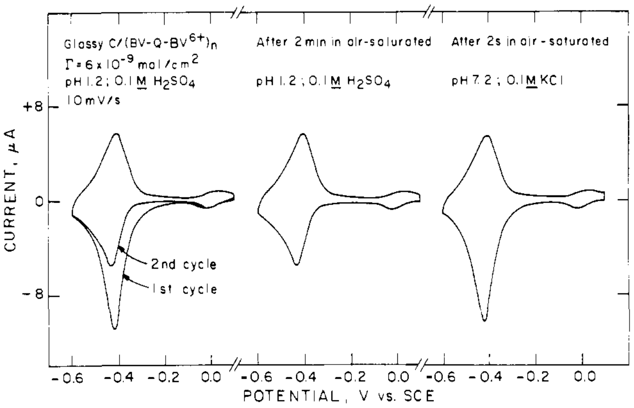

Figure 3. Demonstration of charge release by O_2 at neutral, but not acidic, pH. Cyclic voltammetry of a C/(BV-Q-BV^{6+})$_n$ electrode in pH 1.2/0.1 M H_2SO_4. After the initial cycles on the left, the electrode is in the charge-trapped BV-QH$_2$-BV^{6+} state. The electrode was then soaked in the indicated solutions for the indicated amount of time and another cyclic voltammogram recorded in the pH 1.2 solution.

of the experiment, the relative amounts of charge trapped and released remained fairly constant. On average, the current signal observed upon changing the solution pH from low to high corresponded to 84% of the charge trapped. The reason it was not 100% is probably due to the presence of a small amount of O_2 in the system, which would not interfere significantly with charge trapping at pH 1.2 but would be expected to rapidly oxidize the trapped Q at pH 7.2 (vide infra).

Oxidation of Trapped QH_2 with O_2. Another method to oxidize the QH_2 trapped in (BV-Q-BV^{6+})$_n$ at acidic pH is to add an oxidant to solution, which can chemically oxidize QH_2. One possible oxidant is O_2 because hydroquinones of similar structure are known to react with O_2 to form H_2O_2 (eq 2).[6] This reaction

$$QH_2 + O_2 \rightarrow Q + H_2O_2 \qquad (2)$$

is thermodynamically favorable by ~0.3 V for the QH_2 in BV-QH$_2$-BV^{6+}. However, there appears to be kinetic limitations at acidic pH as shown in Figure 3. After trapping the polymer in the (BV-QH$_2$-BV^{6+})$_n$ state in deoxygenated pH 1.2 solution, the electrode was taken out of potential control and placed in air-saturated pH 1.2 solution for 2 min. Essentially, no oxidation of QH_2 occurs during this period as judged by a second cyclic voltammogram in deoxygenated pH 1.2 solution, which still shows only the BV$^{2+/+}$ wave. However, quickly dipping the electrode in air-saturated pH 7.2 solution leads to complete oxidation of QH_2 since a third cyclic voltammogram at pH 1.2 shows the full Q/QH$_2$ wave. It is the O_2 in the pH 7.2 solution that is mainly responsible for the oxidation of QH_2, because dipping the electrode in deoxygenated pH 7.2 solution leads to only partial oxidation of QH_2. The ~30% oxidation of QH_2, which does occur when the electrode is dipped into deoxygenated pH 7.2 solution, may be due to exposure to O_2 during the transfer between pH 1.2 and 7.2 solutions or to residual O_2 in the "deoxygenated" pH 7.2 solution. In any case, clearly the kinetics of the reaction of QH_2 with O_2 are strongly pH dependent. Slow kinetics for O_2 reduction by QH_2 at low pH have also been observed by other workers.[7]

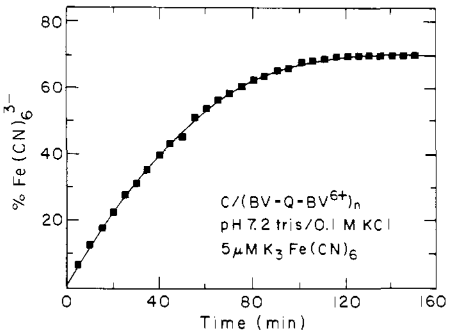

Figure 4. Growth of the amount of electrochemically detectable Fe(CN)$_6^{3-/4-}$ in a (BV-Q-BV^{6+})$_n$-modified electrode as a function of time. (100% incorporation corresponds to 2*n* mol of Fe(CN)$_6^{3-/4-}$ incorporated.) The electrode was held at +0.4 V vs SCE in 100 mL of a stirred 5 μM Fe(CN)$_6^{3-}$ solution in pH 7.2/0.1 M KCl. Cyclic voltammograms from +0.4 to −0.1 V (100 mV/s) were recorded every 5 min to monitor the growth of Fe(CN)$_6^{3-/4-}$.

Charge Release via I_3^-/I^-. Use of irreversible oxidants such as O_2 returns the electrode to the original oxidized (BV-Q-BV^{6+})$_n$ state, but the trapped charge is then associated with the product (H_2O_2) and not returned to the electrode as it is with a pH jump. Another method to oxidize QH_2, which will return charge to the electrode, is to add the reduced form of a reversible couple that when oxidized at the electrode will catalytically oxidize QH_2 (Scheme II). An appropriate compound would have a redox potential positive of the BV$^{2+/+}$ and Q/QH$_2$ couples so trapping could still take place in its presence. An example of such a species is I^-. Figure 1B shows a cyclic voltammogram of the same electrode shown in Figure 1A in a pH 1.2 solution that contains 150 μM KI. The dashed line shows the first cycle, starting at +0.15 V vs SCE and going to −0.6 V vs SCE then back to +0.15 V. As in Figure 1A complete reduction of the polymer occurs, but only BV$^+$ is oxidized in the return sweep from −0.6 to +0.15 V vs SCE. The second scan (smooth line) confirms this by showing the BV$^{2+/+}$ wave without current for mediated Q reduction. Without I^-, no reoxidation of QH_2 occurs when the electrode is scanned to +0.65 V vs SCE, but in the presence of I^- a wave for QH_2 oxidation occurs at ~+0.5 V vs SCE. This is due to catalytic reoxidation of QH_2 by I_3^- (eq 3). Scanning from +0.15 V to +0.65 V vs SCE, when the polymer is in the fully oxidized (BV-Q-BV^{6+})$_n$ state, reveals the underlying I_3^-/I^- wave.

$$QH_2 + I_3^- \rightarrow Q + 2H^+ + 3I^- \qquad (3)$$

Electrostatic Binding of Fe(CN)$_6^{3-/4-}$ in (BV-Q-BV^{6+})$_n$. Fe(CN)$_6^{3-/4-}$ is an example of another reversible redox couple that can catalyze oxidation of QH_2 in (BV-QH$_2$-BV^{6+})$_n$. Fe(CN)$_6^{3-/4-}$ differs from I^- in that, like other large multicharged inorganic anions, it will concentrate in polycationic polymers like (BV-Q-BV^{6+})$_n$.[8-10] Indeed, we find that solution concentrations on the order of 1 μM Fe(CN)$_6^{4-}$ in 0.2 M Cl$^-$ lead to catalytically

---

(6) Calabrese, G. C.; Buchanan, R. M.; Wrighton, M. S. *J. Am. Chem. Soc.* **1983**, *105*, 5594. (b) Smith, D. K.; Wrighton, M. S., unpublished results.

(7) (a) Nagaoka, T.; Sakai, T.; Ogura, K.; Yoshino, T. *Anal. Chem.* **1986**, *58*, 1953. (b) Degrand, C. *J. Electroanal. Chem. Interfacial Electrochem.* **1984**, *169*, 259.

(8) (a) Sumi, K.; Anson, F. C. *J. Phys. Chem.* **1986**, *90*, 3845. (b) Simon, R. A.; Mallouk, T. E.; Daube, K. A.; Wrighton, M. S. *Inorg. Chem.* **1985**, *24*, 3119. (c) Montgomery, D. D.; Shigehara, K.; Tsuchida, E.; Anson, F. C. *J. Am. Chem. Soc.* **1984**, *106*, 7991. (d) Mortimer, R. J.; Anson, F. C. *J. Electroanal. Chem. Interfacial Electrochem.* **1982**, *137*, 149. (e) Kuo, K.; Murray, R. W. *J. Electroanal. Chem. Interfacial Electrochem.* **1982**, *137*, 149. (f) Oyama, N.; Shimomura, T.; Shigehara, K.; Anson, F. C. *J. Electroanal. Chem. Interfacial Electrochem.* **1980**, *112*, 171. (g) Oyama, N.; Anson, F. C. *J. Electrochem. Soc.* **1980**, *127*, 247.

(9) Dominey, R. N.; Lewis, T. J.; Wrighton, M. S. *J. Phys. Chem.* **1983**, *87*, 5345. (b) Bruce, J. A.; Wrighton, M. S. *J. Am. Chem. Soc.* **1982**, *104*, 74.

(10) Mortimer, R. J.; Anson, F. C. *J. Electroanal. Chem. Interfacial Electrochem.* **1982**, *138*, 325.

Table II. DC^2 Values Determined from the Diffusion-Limited Reduction of $Fe(CN)_6^{3-}$ Bound in an Electrode-Confined $(BV\text{-}Q\text{-}BV^{6+})_n$ Film at pH 7.2[a]

electrode no.	$\Gamma(BV\text{-}Q\text{-}BV^{6+})$, mol/cm²	$\Gamma(Fe(CN)_6^{3-})$, mol/cm²	$[Fe(CN)_6^{3-}]$,[c] mol/cm³	DC^2, mol²/s·cm⁴	D, cm²/s
1	9.0×10^{-9}	9.9×10^{-9}	6.6×10^{-4}	1.7×10^{-16}	3.9×10^{-10}
2	9.1×10^{-9}	1.2×10^{-9}	7.9×10^{-5}	2.2×10^{-17}	3.3×10^{-9}
2	9.1×10^{-9}	1.6×10^{-9}	1.1×10^{-4}	2.7×10^{-17}	2.4×10^{-9}
2	9.1×10^{-9}	2.0×10^{-9}	1.3×10^{-4}	3.2×10^{-17}	1.8×10^{-9}
3	6.0×10^{-9}	7.3×10^{-10}	7.3×10^{-5}	5.1×10^{-18}	9.8×10^{-10}
3	6.0×10^{-9}	1.5×10^{-9}	1.5×10^{-4}	2.3×10^{-17}	9.3×10^{-10}
3	6.0×10^{-9}	2.5×10^{-9}	2.5×10^{-4}	3.9×10^{-17}	8.4×10^{-10}
3	6.0×10^{-9}	3.4×10^{-9}	3.4×10^{-4}	4.9×10^{-17}	1.1×10^{-10}
4	5.0×10^{-9}	4.7×10^{-9}	5.6×10^{-4}	7.8×10^{-17}	1.7×10^{-10}
5	1.8×10^{-9}	6.0×10^{-10}	2.1×10^{-4}	9.6×10^{-18}	2.3×10^{-10}
5	1.8×10^{-9}	1.0×10^{-9}	3.6×10^{-4}	2.7×10^{-17}	2.0×10^{-10}
5	1.8×10^{-9}	1.5×10^{-9}	5.3×10^{-4}	3.5×10^{-17}	1.3×10^{-10}

[a] Potential step: +0.40 to +0.10 V vs SCE; DC^2 determined from the slope of the diffusion-limited current vs $t^{-1/2}$ (eq 4). [b] Glassy-carbon electrode; area = 0.071 cm². [c] Concentration of $Fe(CN)_6^{3-}$ in $(BV\text{-}Q\text{-}BV^{6+})_n$, determined by assuming 0.6 M for the concentration of $BV\text{-}Q\text{-}BV^{6+}$ monomer units in the polymer film.

significant amounts of $Fe(CN)_6^{3-/4-}$ incorporated into the polymer. Figure 4 illustrates the growth of the $Fe(CN)_6^{3-/4-}$ wave as a function of time for a $C/(BV\text{-}Q\text{-}BV^{6+})_n$ electrode (coverage, 1.2×10^{-8} mol/cm²) in a 2 μM $Fe(CN)_6^{3-}$/0.2 M Cl^- solution. The wave levels off after 2 h at a $Fe(CN)_6^{3-/4-}$ incorporation of $1.43n$ ($2.0n$ incorporation would result from complete charge compensation of n moles of $BV\text{-}Q\text{-}BV^{6+}$ by $Fe(CN)_6^{3-}$, i.e., a 2:1 molar ratio of $Fe(CN)_6^{3-}$ to $BV\text{-}Q\text{-}BV^{6+}$). Since the concentration of monomer units within the polymer is between 0.4 and 0.8 M,[1b] depending upon the degree of solvent swelling, the concentration of $Fe(CN)_6^{3-/4-}$ in the polymer is on the order of 0.1–1.0 M, a 10^5–10^6-fold increase over the $Fe(CN)_6^{4-}$ concentration in solution. Because of this, it does not actually matter whether $Fe(CN)_6^{4-}$ or $Fe(CN)_6^{3-}$ is added to solution. The concentration of material in solution is insignificant relative to that in the polymer, and the oxidation state of the bound $Fe(CN)_6^{3-/4-}$ is controlled by the electrode.

Although the results in Figure 4 are typical, other electrodes do give slightly different results, making it difficult to quantify the equilibrium between solution and polymer-bound $Fe(CN)_6^{3-/4-}$. In general, if a large, stirred volume of solution is used, a $Fe(CN)_6^{3-/4-}$ concentration of 2 μM in pH 7.2/0.2 M KCl results in significant, but less than complete, charge compensation of the polycation by the $Fe(CN)_6^{3-/4-}$. A solution concentration of >5 μM $Fe(CN)_6^{3-/4-}$ ensures nearly complete charge compensation.

The $Fe(CN)_6^{3-/4-}$-loaded polymer gradually loses a significant fraction of the bound complex when the electrode is placed in solution containing no added $Fe(CN)_6^{3-/4-}$. Upon cycling the potential to reduce the BV^{2+} units the metal complex is lost more rapidly from the polymer and more rapidly than in experiments with analogous pure viologen films.[9,10]

Although there are small differences in the binding of $Fe(CN)_6^{3-/4-}$ in $(BV\text{-}Q\text{-}BV^{6+})_n$ compared to pure viologen polymers, $E°'(Fe(CN)_6^{3-/4-})$ in $(BV\text{-}Q\text{-}BV^{6+})_n$, as with the pure viologen polymers,[9,10] is within 50 mV of $E°'(Fe(CN)_6^{3-/4-})$ in aqueous electrolyte. In addition, the temperature dependence of $E°'(Fe(CN)_6^{3-/4-})$ in $(BV\text{-}Q\text{-}BV^{6+})_n$ is similar to the temperature dependence of $Fe(CN)_6^{3-/4-}$ in aqueous electrolyte. At 25 °C, the aqueous 0.5 mM $Fe(CN)_6^{3-/4-}$ redox potential, as measured by the average potential of the oxidation and reduction peak currents, is 0.202 V vs SCE and moves from 0.234 to 0.168 V vs SCE as the temperature is increased from 3 to 47 °C. Similarly, $Fe(CN)_6^{3-/4-}$ in $(BV\text{-}Q\text{-}BV^{6+})_n$ has redox potentials of 0.176, 0.149, and 0.121 V vs SCE at 3, 25, and 47 °C, respectively. The temperature dependence of $E°'$ is greater than 1 mV/°C for the aqueous redox potential of $Fe(CN)_6^{3-/4-}$. This is substantially larger than that found for the majority of redox couples and has been attributed to the large entropies of solvation for the $Fe(CN)_6^{3-}$ and $Fe(CN)_6^{4-}$ ions.[11] The magnitude of the temperature dependence of $E°'(Fe(CN)_6^{3-/4-})$ is almost as large within the loaded $(BV\text{-}Q\text{-}BV^{6+})_n$ as in the aqueous medium.

Apparent diffusion coefficients for charge transport, D, of $Fe(CN)_6^{3-/4-}$ in $(BV\text{-}Q\text{-}BV^{6+})_n$ can be determined from the current–time response following a potential step resulting in reduction of $Fe(CN)_6^{3-}$.[10,12] For diffusion-controlled situations, the current response is predicted by the Cottrell equation (eq 4),

$$i = nFAD^{1/2}C/(\pi^{1/2}t^{1/2}) \tag{4}$$

where n is the number of moles of electrons per center, F is Faraday's constant, A is the area of the electrode, D is the diffusion coefficient, and C is the concentration of diffusing species. Values of DC^2 determined from slopes of the linear i vs $t^{-1/2}$ plots for several $C/(BV\text{-}Q\text{-}BV^{6+})_n$ electrodes with different $Fe(CN)_6^{3-/4-}$ incorporations are listed in Table II. Values of D were calculated from the DC^2 values, assuming the concentration of monomer units in the polymer equals 0.6 M and the concentration of $Fe(CN)_6^{3-/4-}$, C, equals the incorporation level times 0.6 M.[1b] The resulting D values are 3–4 orders of magnitude smaller than the value for the diffusion coefficient of $Fe(CN)_6^{3-}$ in aqueous solution, 7×10^{-6} cm²/s,[12] but similar to the values that have been reported for $Fe(CN)_6^{3-}$ in another viologen-based polycationic polymer.[10] Values of D given in Table II have an error of ±20%, owing to uncertainty in C.

The general trend appears to be that D decreases as the $Fe(CN)_6^{3-/4-}$ loading within the polymer increases. This probably reflects an increasing rigidity of the polymer caused by additional electrostatic cross-linking. This should lower electron self-exchange and movement of the redox centers in the polymer, leading to lower values of D. Increased $Fe(CN)_6^{3-/4-}$ incorporation has similar deleterious effects on the polymer electrochemistry. Under all conditions, increased levels of $Fe(CN)_6^{3-/4-}$ lead to more sluggish electrochemical processes in $(BV\text{-}Q\text{-}BV^{6+})_n$. The bound $Fe(CN)_6^{3-/4-}$ results in smaller $(BV\text{-}Q\text{-}BV^{6+})_n$ peaks at a given scan rate and larger peak-to-peak separations. Similar effects have been previously noted with the incorporation of $Fe(CN)_6^{3-/4-}$ and other large anions in viologen-based polymers.[9,10]

Charge Release via $Fe(CN)_6^{3-/4-}$. Figure 5 shows the cyclic voltammetry of a $C/(BV\text{-}Q\text{-}BV^{6+})_n$ electrode in 10 μM $Fe(CN)_6^{3-}$, pH 7.2/0.1 M KCl. The set of waves centered at 0.2 V vs SCE corresponds to the oxidation and reduction of $Fe(CN)_6^{4-/3-}$ in the polymer, and those at −0.35 and −0.5 V vs SCE correspond to Q/QH_2 and $BV^{2+/+}$, respectively. Note that, unlike in pH 1.2 electrolyte, the reduction of Q occurs near the thermodynamic potential and is reasonably reversible. At the slowest scan rate, 10 mV/s, the Q/QH_2 reduction peak is completely separate from the $BV^{2+/+}$ reduction peak. At faster scan rates, however, the two cathodic peaks merge and the anodic Q/QH_2 peak decreases in size relative to the $BV^{2+/+}$ anodic peak. Further, it is evident

---

(11) Hanania, G. I. H.; Irvine, D. H.; Eaton, W. A.; George, P. *J. Phys. Chem.* **1967**, *71*, 2022.

(12) Daum, P.; Lenhard, J. R.; Robinson, D. R.; Murray, R. W. *J. Am. Chem. Soc.* **1980**, *102*, 4649.

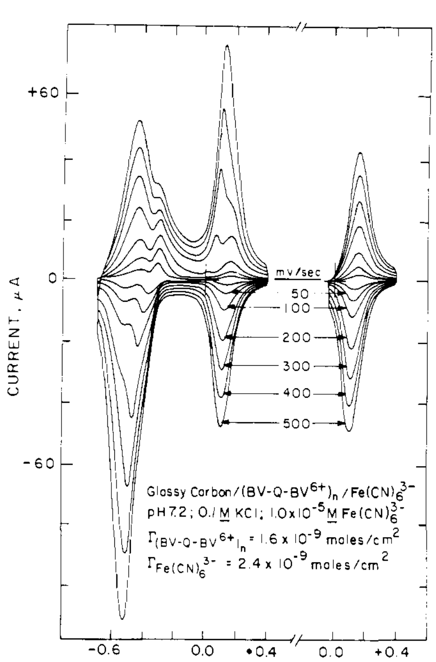

Figure 5. Cyclic voltammetry at different scan rates for a C/(BV-Q-BV^{6+})$_n$ electrode with 1.5n mol of Fe(CN)$_6^{3-/4-}$ incorporation in pH 7.2/0.1 M KCl. Catalytic oxidation of QH$_2$ is evident from the excess current in the anodic Fe(CN)$_6^{3-/4-}$ waves.

that the area of the cathodic peak is larger than the anodic peak. The relatively slow QH$_2$ oxidation is consistent with mediated, but slow, oxidation of QH$_2$ by BV^{2+} even at this pH. Reduction of the Q centers by the BV$^+$ units is expected to be faster than the oxidation of the QH$_2$ centers by BV^{2+}, since reduction of Q is still a slightly energetically downhill process at pH 7.2, while oxidation of QH$_2$ is a slightly energetically uphill process.

The incomplete oxidation of QH$_2$ by BV^{2+} at fast scan rates in pH 7.2 solution allows demonstration of Fe(CN)$_6^{3-/4-}$-mediated QH$_2$ oxidation even at this, nonrectifying, pH. Comparison of the two sets of cyclic voltammograms in Figure 5 shows excess current in the anodic portion of the Fe(CN)$_6^{3-/4-}$ wave after cycling through the (BV-Q-BV^{6+})$_n$ waves. In fact, starting with the 100 mV/s scan, a "prewave" is seen on the negative side of the Fe(CN)$_6^{3-/4-}$ anodic wave. This prewave corresponds to catalytic oxidation of QH$_2$ by Fe(CN)$_6^{3-}$ (eq 5). As the scan rate is increased, the size of this prewave increases and shifts positive, closer to the Fe(CN)$_6^{3-/4-}$ peak.

$$QH_2 + 2Fe(CN)_6^{3-} \rightarrow Q + 2H^+ + 2Fe(CN)_6^{4-} \quad (5)$$

Due to the adverse effects of high levels of Fe(CN)$_6^{3-/4-}$ incorporation on the (BV-Q-BV^{6+})$_n$ electrochemistry, it would be better to use low levels to catalyze charge release from (BV-QH$_2$-BV^{6+})$_n$ at low pH. Fortunately, low levels of Fe(CN)$_6^{3-/4-}$ incorporation are adequate to catalyze complete charge release. Figure 6 shows a cyclic voltammogram of a C/(BV-Q-BV^{6+})$_n$ electrode with approximately 0.1n Fe(CN)$_6^{3-/4-}$ in pH 1.2 electrolyte. The results are similar to those obtained with 150 μM I$^-$ in solution (Figure 1B).

The kinetics of the Fe(CN)$_6^{3-/4-}$-mediated charge release at pH 1.2 was examined qualitatively by looking at the sweep-rate dependence of the cyclic voltammetry (Figure 7). On the left, scans were recorded between +0.5 and −0.6 V vs SCE. The rates of the Fe(CN)$_6^{3-/4-}$ interconversions are much faster than the rates of the BV$^{2+/+}$ interconversions. The (BV-QH$_2$-BV^{6+})$_n$ peak currents are not proportional to scan rate, even at rates as slow as 50 mV/s, while the peak currents of the polymer-bound Fe(CN)$_6^{3-/4-}$ waves (inset) are proportional to scan rate up to 200 mV/s. The lack of a diffusional tail on the positive side of the Fe(CN)$_6^{3-/4-}$ anodic waves after catalytic charge release suggests that the Fe(CN)$_6^{3-/4-}$ is able to mediate the full oxidation of that portion of the polymer that was reduced. However, the presence of a significant diffusional tail on the negative side of the polymer cathodic waves indicates that not all of the polymer was reduced at the faster scan rates.

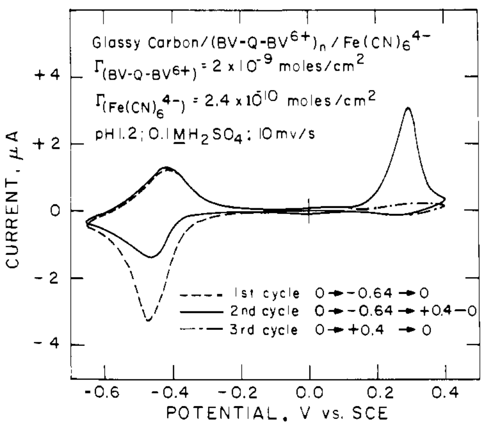

Figure 6. Demonstration of mediated charge release by Fe(CN)$_6^{3-/4-}$. Cyclic voltammetry of a C/(BV-Q-BV^{6+})$_n$ electrode with 0.1n mol of Fe(CN)$_6^{3-/4-}$ incorporation in pH 1.2/0.1 M H$_2$SO$_4$.

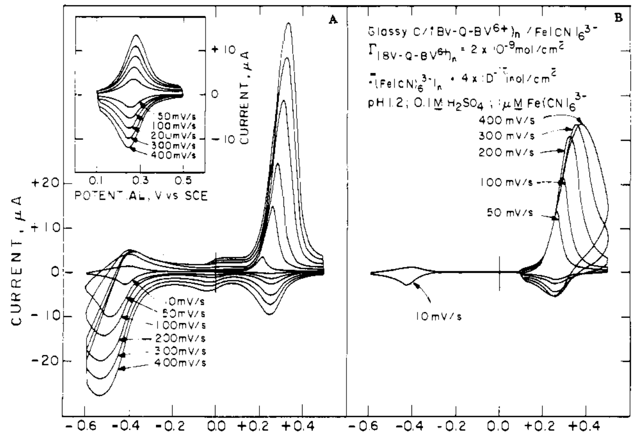

Figure 7. Cyclic voltammetry at different sweep rates of a C/(BV-Q-BV^{6+})$_n$ electrode with 0.2n mol of Fe(CN)$_6^{3-/4-}$ incorporation in pH 1.2/0.1 M H$_2$SO$_4$. (A) On the left, the scans were recorded between +0.5 and −0.6 V vs SCE. The inset shows cyclic voltammetry of only the Fe(CN)$_6^{3-/4-}$ system. (B) On the right, the electrode was cycled at 10 mV/s between +0.1 and −0.6 V before each scan through the wave for Fe(CN)$_6^{3-/4-}$. This ensured that the polymer was initially in the charge-trapped (BV-QH$_2$-BV^{6+})$_n$ state.

In order to eliminate the complications arising from slow polymer kinetics, cyclic voltammograms of the Fe(CN)$_6^{3-/4-}$ wave were also recorded from +0.1 to +0.5 V vs SCE after the electrode had been initially cycled at 10 mV/s from +0.1 to −0.6 V (Figure 7B). This ensured that the electrode was in the partially reduced (all Q centers in QH$_2$ state), charge-trapped (BV-QH$_2$-BV^{6+})$_n$ state at the beginning of each scan from +0.1 to +0.5 V vs SCE. This technique produces quite different results than cycling through both the polymer and Fe(CN)$_6^{3-/4-}$ waves at the same scan rate. The Fe(CN)$_6^{3-}$ is able to oxidize all of the QH$_2$ up to 100 mV/s, but severe kinetic limitations set in between 200 and 300 mV/s. The amount of charge associated with the mediated oxidation of the polymer in Figure 7B is significantly less than that associated with the mediated oxidation of the polymer in Figure 7A at each scan rate. This suggests that a possible limiting factor in the charge-release process is the structural reorganization that accompanies the change from the partially reduced, charge-trapped (BV-QH$_2$-BV^{6+})$_n$ state to the completely oxidized (BV-Q-BV^{6+})$_n$ state. When potential cycles are started with the polymer in its fully oxidized state (Figure 7A), the polymer reorganization involved in the transition is apparently not complete, making it easier to go back to the completely oxidized state than when the cycles are started from the charge-trapped state, as reflected in the larger peak currents for the

$Fe(CN)_6^{3-/4-}$-mediated currents.

Another possible explanation for the differences between parts A and B of Figure 7 is that the greater current observed on the $Fe(CN)_6^{3-/4-}$ oxidation wave in Figure 7A is due to BV^+ also being catalytically oxidized by $Fe(CN)_6^{3-}$. In support of this argument, the $BV^{2+/+}$ cathodic wave does not increase in size between 100 and 400 mV/s, indicating that only a fraction of the possible amount of BV^+ present is being directly oxidized at fast scan rates. However, the small BV^+ oxidation wave in Figure 7A could also be due to the fact that not all of the $BV^{2+/+}$ is in the BV^+ state at the end of the fast negative sweeps, because the BV^+ is still being catalytically turned over by Q.

If we assume, nonetheless, that the limiting $Fe(CN)_6^{3-/4-}$ oxidation current observed in Figure 7B is due to the rate of oxidation of QH_2 by $Fe(CN)_6^{3-}$ and not due to structural reorganization in the polymer, then a value for the rate constant of this reaction can be estimated from this data. Successive steps of (i) electron transfer, (ii) deprotonation, (iii) electron transfer, and (iv) deprotonation have been observed for the aqueous oxidation of QH_2 in the low-pH range,[13] with the first electron transfer step being rate limiting. We consider an analogous mechanism (eq 6–9),

$$QH_2 + Fe(CN)_6^{3-} \rightleftarrows QH_2^{\bullet +} + Fe(CN)_6^{4-} \tag{6}$$

$$QH_2^{\bullet +} \rightleftarrows QH^{\bullet} + H^+ \tag{7}$$

$$QH^{\bullet} + Fe(CN)_6^{3-} \rightleftarrows QH^+ + Fe(CN)_6^{4-} \tag{8}$$

$$QH^+ \rightleftarrows Q + H^+ \tag{9}$$

for the oxidation of QH_2 centers by $Fe(CN)_6^{3-}$ within $(BV\text{-}QH_2\text{-}BV^{6+})_n$. Assuming that the electron transfer represented by eq 6 is rate determining, the rate equation for the oxidation of QH_2 by $Fe(CN)_6^{3-}$ is given by eq 10. The rate constant, k_2,

$$-d[QH_2]/dt = k_2[QH_2][Fe(CN)_6^{3-}] \tag{10}$$

may therefore be expressed by eq 11. As seen in Figure 7B, complete oxidation of QH_2 is limited to a scan rate of approximately 200 mV/s. At this scan rate, available QH_2 and $Fe(CN)_6^{4-}$ are consumed within 2 s. If at a potential halfway through the oxidation wave half the estimated available 0.6 M QH_2 and 0.12 M $Fe(CN)_6^{4-}$ are oxidized, then, from eq 11, the order of magnitude of the rate constant for $Fe(CN)_6^{3-/4-}$ oxidation of QH_2 is given by:

$$k_2 = \{d[QH_2]/dt\}/\{[QH_2][Fe(CN)_6^{3-}]\} \tag{11}$$

$$k_2 \sim (0.6\ M/2\ s)/[(0.5 \times 0.6\ M)(0.5 \times 0.12\ M)] \approx 2 \times 10^1\ M^{-1}\ s^{-1}$$

Conclusions

Two types of systems have been demonstrated in which a controllable outside signal triggers release of charge trapped in $(BV\text{-}QH_2\text{-}BV^{6+})_n$ at low pH, enabling the charge to be collected at the electrode. In the first example the signal is a pH change from low to high pH (Scheme I). This shifts $E^{\circ\prime}(Q/QH_2)$ negative, allowing equilibration of the QH_2 with the $BV^{2+/+}$ system, through which the charge is returned to the electrode. The second charge-release scheme employs an additional redox couple to mediate the transfer of charge from the Q/QH_2 system to the electrode at low pH (Scheme II). In this case the signal is a change in electrode potential from negative of $E^{\circ\prime}$ of the mediator to positive of $E^{\circ\prime}$ of the mediator. This triggers release of trapped charge by oxidizing the mediator, which, in turn, oxidizes the QH_2.

Mediation by $Fe(CN)_6^{3-/4-}$ was examined in the greatest detail because of the strong electrostatic binding of $Fe(CN)_6^{3-/4-}$ in polycations like $(BV\text{-}Q\text{-}BV^{6+})_n$.[8-10] Not surprisingly, we find that $Fe(CN)_6^{3-/4-}$ in $(BV\text{-}Q\text{-}BV^{6+})_n$ behaves in many respects like $Fe(CN)_6^{3-/4-}$ in other viologen-based polycations. There is some indication that $Fe(CN)_6^{3-/4-}$ does not bind as strongly to $(BV\text{-}Q\text{-}BV^{6+})_n$ as it does to the other viologen polymers, because reduction of BV^{2+} to BV^+ leads to expulsion of $Fe(CN)_6^{3-/4-}$ from $(BV\text{-}Q\text{-}BV^{6+})_n$ but not from pure $BV^{2+/+}$-based polymers.[9,10] However, apparent D values of $Fe(CN)_6^{3-}$ in $(BV\text{-}Q\text{-}BV^{6+})_n$ are similar to those reported for $Fe(CN)_6^{3-}$ in viologen polymers.[10] Also, the effect of $Fe(CN)_6^{3-/4-}$ on the viologen electrochemistry is similar. With both $(BV\text{-}Q\text{-}BV^{6+})_n$ and the other viologen polymers the presence of $Fe(CN)_6^{3-/4-}$ leads to slower electrochemical interconversion of BV^{2+} and BV^+. Fortunately, small amounts of $Fe(CN)_6^{3-/4-}$, which have minimal effect on the $BV^{2+/+}$ electrochemistry, can catalyze the release of trapped charge in $(BV\text{-}Q\text{-}BV^{6+})_n$ with reasonable rates.

Both the $Fe(CN)_6^{3-/4-}/(BV\text{-}Q\text{-}BV^{6+})_n$ and pH jump schemes achieve the desired goal of releasing the charge trapped in $(BV\text{-}QH_2\text{-}BV^{6+})_n$ at low pH and returning the charge to the electrode. Beyond that, both schemes are also interesting from a purely conceptual point of view. The pH jump scheme exhibits a unique effect, because, rather than measuring a change in chemical concentration by a change in solution potential or a change in conductivity, the pH jump, in effect, converts a chemical concentration change directly to an electrical current. The $Fe(CN)_6^{3-/4-}/(BV\text{-}Q\text{-}BV^{6+})_n$ system is also unique because it represents a three-component modified-electrode assembly in which each component has a separate but necessary role to play in order to achieve the overall function.

Acknowledgment. We thank the United States Department of Energy, Office of Basic Energy Sciences, Division of Chemical Sciences, for support of this research.

Registry No. $(BV\text{-}Q\text{-}BV)_n^{6+}$, 112795-44-5; C, 7440-44-0; I_3^-, 14900-04-0; I^-, 20461-54-5; $Fe(CN)_6^{4-}$, 13408-63-4; $Fe(CN)_6^{3-}$, 13408-62-3.

---

[13] Laviron, E. *J. Electroanal. Chem. Interfacial Electrochem.* **1984**, *164*, 213.